

## Universal energy-accuracy tradeoffs in nonequilibrium cellular sensing

Sarah E. Harvey <sup>\*</sup>, Subhaneil Lahiri , and Surya Ganguli

*Department of Applied Physics, Stanford University, Stanford, California 94305, USA*



(Received 15 November 2022; accepted 7 April 2023; published 7 July 2023)

We combine stochastic thermodynamics, large deviation theory, and information theory to derive fundamental limits on the accuracy with which single cell receptors can estimate external concentrations. As expected, if the estimation is performed by an ideal observer of the entire trajectory of receptor states, then no energy consuming nonequilibrium receptor that can be divided into bound and unbound states can outperform an equilibrium two-state receptor. However, when the estimation is performed by a simple observer that measures the fraction of time the receptor is bound, we derive a fundamental limit on the accuracy of general nonequilibrium receptors as a function of energy consumption. We further derive and exploit explicit formulas to numerically estimate a Pareto-optimal tradeoff between accuracy and energy. We find this tradeoff can be achieved by nonuniform ring receptors with a number of states that necessarily increases with energy. Our results yield a thermodynamic uncertainty relation for the time a physical system spends in a pool of states and generalize the classic Berg-Purcell limit [H. C. Berg and E. M. Purcell, *Biophys. J.* **20**, 193 (1977)] on cellular sensing along multiple dimensions.

DOI: [10.1103/PhysRevE.108.014403](https://doi.org/10.1103/PhysRevE.108.014403)

### I. INTRODUCTION

Single cells possess extremely sensitive mechanisms for detecting chemical concentrations through the binding of molecules to cell-surface receptors (Fig. 1(a), Refs. [1–5]) and can use this information to respond to external concentration signals. The phenomenon of a cell initiating directional motion in response to a chemical signal is called chemotaxis and is widely observed in prokaryotic cells searching the environment, as well as in eukaryotic cell motion that occurs, for example, in immune responses and cancer cell metastasis [6,7]. At a more abstract level, the relationship between information and thermodynamics has been studied in many physical contexts [8–13], which has naturally lead to questions about the fundamental limits that energy consumption places on biological information processing [14–16]. The remarkable capacity of cells to sense their environment may require energy consumption, for example, through the use of G-protein coupled receptors that cycle through multiple states [17–20]. This suggests that there could exist theoretical limits on the accuracy of cellular chemosensation, as a function of both the energy consumed by arbitrarily complex nonequilibrium receptors and the computational sophistication of downstream observers of these dynamics.

A seminal line of work by Berg and Purcell in 1977 [21–23] addressed this question for equilibrium receptors described by two states, bound and unbound, with the binding transition rate proportional to the external concentration  $c$  [Fig. 1(b)]. Berg and Purcell studied the accuracy of a concentration estimate  $\hat{c}$  computed by a simple observer (SO)

that only has access to the fraction of time the receptor is bound over a time  $T$ , finding a fundamental lower bound on the fractional error of this estimate:

$$\epsilon_{\hat{c}}^2 \equiv \frac{\langle(\delta\hat{c})^2\rangle}{c^2} \geq \frac{2}{\bar{N}}. \quad (1)$$

Here  $\langle(\delta\hat{c})^2\rangle$  is the variance of the estimate  $\hat{c}$ , and  $\bar{N}$  is the mean number of binding events in time  $T$ .

For over 30 years, Eq. (1) was thought to constitute a fundamental physical limit on the accuracy of cellular chemosensation. However, recent work focusing on highly specific receptor models [15,24–26] revealed this limit could be circumvented in two qualitatively distinct ways. First, in the simple case of a two-state receptor, an ideal observer (IO) that has access to the entire receptor trajectory of binding and unbinding events could outperform the SO by performing a maximum-likelihood estimate, obtaining an error of  $\epsilon_{\hat{c}}^2 = \frac{1}{\bar{N}}$  [25]. The IO in this case outperforms the SO by a factor of 2, which is achieved by measuring the mean duration of unbound intervals and ignoring the duration of bound intervals. Ignoring the bound intervals improves performance because the transition rate out of the bound state is independent of  $c$ , and so the bound interval time simply contributes spurious noise. Second, even when the estimate is performed by a SO, the Berg-Purcell limit can be overcome by energy-consuming nonequilibrium receptors with more than two states [Fig. 1(d)], potentially reflecting different receptor conformations or phosphorylation states [24–26]. Notably, Lang *et al.* [26] numerically observed a tradeoff between error and energy for a very specific class of receptor models with states arranged in a ring.

While these more recent works demonstrate circumventions of the Berg-Purcell limit in highly specific models, they leave open foundational theoretical questions about the

<sup>\*</sup>harveys@stanford.edu

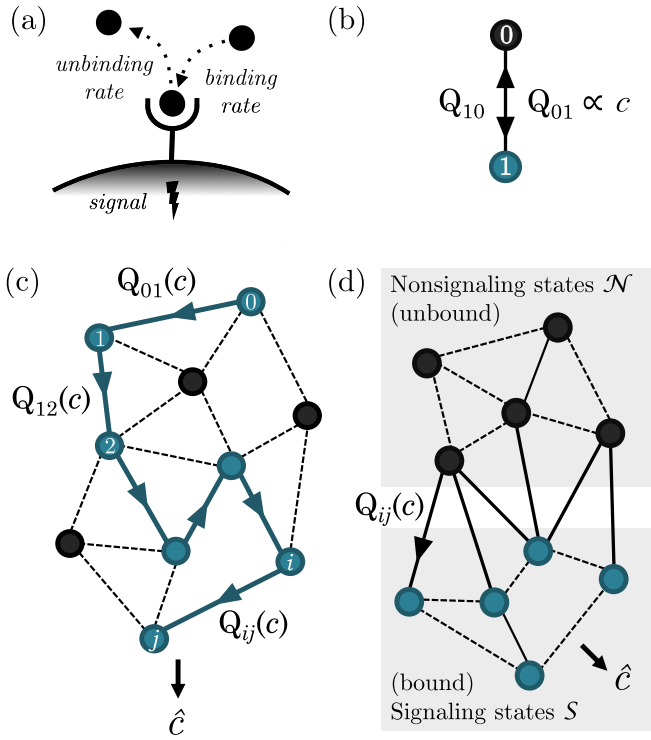


FIG. 1. Cells employ many membrane-bound receptors in order to form an estimate of an external concentration relevant to its behavior. Single receptors may be modeled as continuous-time Markov processes. (a) Cartoon of a single receptor. (b) Single receptor modeled as a two-state continuous-time Markov process (Berg-Purcell model) with binding rate  $Q_{01}$  and unbinding rate  $Q_{10}$ . (c) and (d) Generalizing to many-state processes. (c) An ideal observer uses the process trajectory to form an estimate  $\hat{c}$  of the concentration signal  $c$ , which modulates the receptor’s transition rates  $Q_{ij}(c)$ . (d) A simple observer measures the fraction of time the receptor spends in a subset of states (“signaling states”) to estimate the signal.

general interplay between estimation accuracy and energy consumption across the large space of possible complex nonequilibrium receptors.

In particular, what are the fundamental limits of sensing accuracy for the IO and what computation must the IO perform on the receptor trajectory of complex receptors to achieve this limit? Also for a SO can we derive general *analytic* bounds or exact formulas for accuracy in terms of energy expenditure for general classes of nonequilibrium receptors? Can we exploit these formulas to find Pareto-optimal receptors through numerical optimization?

We address these questions by combining and extending stochastic thermodynamics [27–32] and large deviation theory (LDT) of Markov chains [33–39]. We derive a thermodynamic uncertainty relation connecting fluctuations in the time a stochastic process occupies a subset of states and the energy dissipated by that process. This relation is of independent interest in nonequilibrium statistical mechanics [38–41] and could have applications not only in cellular chemosensation, as discussed here, but also in understanding relations between energy dissipation and accuracy or robustness in other

biological processes, like cellular motors and biological clocks [42–44].

## II. OVERALL FRAMEWORK

A general nonequilibrium receptor can be modeled as a continuous-time Markov process [10,26], with  $n$  different conformational or signaling states indexed by  $i = 0, \dots, n - 1$ . As in Ref. [26], we focus on modeling the receptor and we neglect the complex downstream cellular machinery that converts the receptor output into a behavior [2]. The transition rate from state  $i$  to state  $j$  is  $Q_{ij}$ . We assume some subset of these rates correspond to binding transitions with rates proportional to the concentration  $c$  (see Sec. VII of the Supplemental Material [45] for a discussion of a more complex dependency on concentration). Over an observation time  $T$ , the receptor then moves randomly through a sequence of states  $\{x_0, x_1, \dots, x_m\}$  with transitions out of each state  $x_k \in \{0, \dots, n - 1\}$  occurring at random times  $0 \leq t_k \leq T$ , yielding a stochastic trajectory  $x(t)$  with  $x(t) = x_k$  for  $t_{k-1} \leq t < t_k$ . An IO that has access to the entire trajectory [Fig. 1(c)] can compute a maximum likelihood estimate  $\hat{c}$  of the concentration  $c$  via

$$\hat{c} = \operatorname{argmax}_c \log \mathbb{P}[x(t)|c], \quad (2)$$

where  $\mathbb{P}[x(t)|c]$  denotes the probability distribution over receptor-state trajectories at a given concentration  $c$ . To discuss the SO, we further assume that binding transitions occur from a group of states defined as unbound, nonsignaling states,  $\mathcal{N}$ , to states we call the bound, signaling states,  $\mathcal{S}$  [Fig. 1(d)]. While an IO can access information contained in the entire trajectory  $x(t)$ , we assume the SO can only measure the fraction of time spent in the signaling states. While we study both the IO and the SO, in this work we focus primarily on the SO, as this model of observation can be plausibly implemented, for example, by counting the number of second messengers generated during the interval of time the receptor is bound. In contrast, it is unclear mechanistically how an IO could be realized. We note overall that our assumptions are consistent with previous work [25,26], though they exclude receptors with intermediate states that are bound but not signaling [46].

## III. RECEPTOR COMPLEXITY AND THE IDEAL OBSERVER

We first ask if it is possible to improve the estimation accuracy of an IO through the addition of more states and transitions beyond the two-state process [25]. The properties of continuous-time Markov processes (see Appendix B of Ref. [45]) imply the log probability of trajectory  $x(t)$  reduces to [34–37]

$$\log \mathbb{P}[x(t)|c] = -T \sum_{i \neq j} [p_i^T Q_{ij} - \phi_{ij}^T \log Q_{ij}], \quad (3)$$

where  $p_i^T$  is the empirical density, or the fraction of total time  $T$  that the trajectory  $x(t)$  spends in state  $i$ , and  $\phi_{ij}^T$  is the empirical flux, or the number of transitions from state  $i$  to state  $j$  along the trajectory  $x(t)$ , divided by  $T$ .

Maximizing Eq. (3) with respect to  $c$  yields the IO estimate  $\hat{c}$  in Eq. (2). When only transition rates from  $\mathcal{N}$  to  $\mathcal{S}$  are proportional to  $c$  as in Fig. 1(d),

$$\hat{c} = \frac{R^T}{R^p|_{c=1}}, \quad (4)$$

where  $R^T \equiv \sum_{i \in \mathcal{N}, j \in \mathcal{S}} \phi_{ij}^T$  is the receptor's empirical binding rate along trajectory  $x(t)$ , and  $R^p \equiv \sum_{i \in \mathcal{N}, j \in \mathcal{S}} p_i^T Q_{ij}$  is the expected binding rate conditioned on the empirical density  $p_i^T$ . For two states,  $\hat{c}$  is inversely proportional to the total duration of unbound intervals, agreeing with Ref. [25]. However, this result generalizes Ref. [25] to reveal what function of a more complex trajectory  $x(t)$  an IO must compute to estimate the concentration for arbitrarily connected receptors, as in Fig. 1(d).

The Cramér-Rao bound [47] gives a lower bound on the fractional error  $\epsilon_{\hat{c}}^2$  of the IO through the Fisher information  $J_c$  of the receptor trajectory  $x(t)$  with respect to the external concentration  $c$ . A simple calculation detailed in Sec. II A of Ref. [45] yields

$$J_c = J_c^0 + T \sum_{i \neq j} \pi_i Q_{ij} [\partial_c \log Q_{ij}]^2. \quad (5)$$

Here  $\pi_i$  is the steady-state probability of state  $i$ , and  $J_c^0 = \sum_i \pi_i (\partial_c \log \pi_i)^2$  is the Fisher information of an observation of the initial state sampled from the steady-state distribution. The term linear in  $T$  reflects additional information obtained from observing an entire trajectory, instead of a single state occupancy. Note only transition rates modulated by  $c$  contribute information. The result in Eq. (5) holds for arbitrary receptors as in Fig. 1(c), but for receptors of the form in Fig. 1(d) with transition rates linear in  $c$ , the result simplifies to

$$J_c = J_c^0 + \frac{T}{c^2} R^\pi, \quad (6)$$

where  $R^\pi = \sum_{i \in \mathcal{N}, j \in \mathcal{S}} \pi_i Q_{ij}$  is the expected steady-state binding rate. Then the Cramér-Rao (CR) bound yields the following for large  $T$ ,

$$\epsilon_{\hat{c}}^2 \equiv \frac{\langle (\delta \hat{c})^2 \rangle}{c^2} \geq \frac{1}{J_c c^2} = \frac{1}{T R^\pi} = \frac{1}{\bar{N}}, \quad (7)$$

where  $\bar{N}$  is the expected number of binding events. In Sec. V A of Ref. [45] we directly calculate the variance of the IO concentration estimate in Eq. (4) and demonstrate that its error saturates the CR bound, Eq. (7). This result generalizes [25] from simple equilibrium two state receptors to arbitrarily connected nonequilibrium receptors of the form in Fig. 1(d), confirming that any such energy-consuming nonequilibrium receptor with binding rates proportional to the concentration cannot outperform an IO of a simple equilibrium two-state receptor.

#### IV. FLUCTUATIONS AND GAIN DETERMINE SIMPLE OBSERVER PERFORMANCE

The IO estimate in Eq. (2) requires computing a complex function of the receptor trajectory  $x(t)$ , which may not be plausibly implementable in biological systems. Therefore, we

next explore a simple observer (SO), which estimates the concentration using only some readout of the fraction of total measurement time  $T$  that the receptor is bound (signaling), which we denote  $q^T = \sum_{i \in \mathcal{S}} p_i^T$ . Due to randomness in  $x(t)$ ,  $q^T$  fluctuates about its mean  $q^\pi = \sum_{i \in \mathcal{S}} \pi_i$ , which depends on the concentration  $c$ . Given the observable  $q^T$ , one can then estimate  $\hat{c}$  by solving for the concentration value that would make this observation of  $q^T$  equal to its expected value  $q^\pi$ , or in essence, solving for  $\hat{c}$  in the equation  $q^\pi(\hat{c}) = q^T$ . Standard error propagation then yields

$$\epsilon_{\hat{c}}^2 = \frac{\langle (\delta \hat{c})^2 \rangle}{c^2} = \left[ c \frac{dq^\pi}{dc} \right]^{-2} \langle (\delta q^T)^2 \rangle. \quad (8)$$

Thus, a larger variance  $\langle (\delta q^T)^2 \rangle$  in the time spent bound increases the error  $\epsilon_{\hat{c}}^2$ , while a larger gain term  $|\frac{dq^\pi}{dc}|$  decreases it. We next compute and bound this variance and gain, leading to a bound on the overall estimation error  $\epsilon_{\hat{c}}^2$ .

#### V. A THERMODYNAMIC UNCERTAINTY RELATION FOR OCCUPANCY TIME

We first derive a lower bound on the variance  $\langle (\delta q^T)^2 \rangle$  using stochastic thermodynamics and LDT [33] of Markov processes. A random trajectory  $x(t)$  of duration  $T$  in a general Markov process will yield an empirical density  $p_i^T$ , or a fraction of time spent in state  $i$ , and an empirical current  $j_{ij}^T = \phi_{ij}^T - \phi_{ji}^T$ , which corresponds to the *net* number of transitions from  $i$  to  $j$  divided by  $T$ . As  $T \rightarrow \infty$ , these random variables will converge to their mean values, corresponding to the steady-state probabilities  $\pi_i = \lim_{T \rightarrow \infty} p_i^T$  and the steady-state currents  $j_{ij}^\pi \equiv \pi_i Q_{ij} - \pi_j Q_{ji} = \lim_{T \rightarrow \infty} j_{ij}^T$ . At large but finite  $T$ , observations of  $p^T$  and  $j^T$  fluctuate about their means, and their joint distribution is known to satisfy a large deviation principle, taking the form  $\mathbb{P}(p^T = p, j^T = j) \propto e^{-TI(p,j)}$  [34–37,45]. Here  $I(p,j)$  is a rate function that achieves its minimum at  $p = \pi$  and  $j = j^\pi$ , and the form of this function describes how fluctuations in  $p^T$  and  $j^T$  are suppressed as  $T$  becomes large. This rate function is known to be

$$I(p,j) = \sum_{i < j} j_{ij} \left( \operatorname{arcsinh} \frac{j_{ij}}{a_{ij}} - \operatorname{arcsinh} \frac{j_{ij}^\pi}{a_{ij}} \right) - \left( \sqrt{a_{ij}^2 + j_{ij}^2} - \sqrt{a_{ij}^2 + j_{ij}^{\pi 2}} \right), \quad (9)$$

where  $a_{ij} \equiv 2\sqrt{p_i p_j Q_{ij} Q_{ji}}$  and  $j_{ij}^\pi \equiv p_i Q_{ij} - p_j Q_{ji}$  [34–37].

Similarly, at large but finite  $T$ , the distribution of the fraction of time spent bound, namely,  $q^T = \sum_{i \in \mathcal{S}} p_i$ , takes the form  $\mathbb{P}(q^T = q) \propto e^{-TI(q)}$ . The rate function  $I(q)$  achieves its minimum at the mean value  $q^\pi \equiv \sum_{i \in \mathcal{S}} \pi_i$  and could be used to study the fluctuations of  $q^T$  around  $q^\pi$ . The variance of  $q^T$  is given by  $1/[TI''(q^\pi)]$  [33], so any upper bound on  $I''(q^\pi)$  will yield a lower bound on the variance of  $q^T$ .

Since the fraction of time spent in a subset of states  $q^T$  is a function of the empirical density over all states  $p_i^T$ , we can obtain  $I(q)$  from the more general rate function  $I(p,j)$  through an application of the contraction principle [33]. The contraction principle states that  $I(q) = \inf_{p,j} I(p,j)$ , subject to the constraints  $\sum_j j_{ij} \forall i$ ,  $\sum_i p_i = 1$ , and  $\sum_{i \in \mathcal{S}} p_i = q$ .

The contraction principle embodies the intuition that the probability of an atypical fluctuation of the occupancy time  $q^T$  achieving the value  $q$  is dominated by the probability of the *most* likely fluctuation in the empirical density and currents that are consistent with the atypical occupancy time  $q$ . Instead of calculating  $I(q) = \inf_{p,j} I(p, j)$  subject to the constraints directly, we can upper bound the minimum by evaluating  $I(p, j)$  for an ansatz of  $j = j^*(q)$  and  $p = p^*(q)$  satisfying the same constraints.

We developed the following ansatz for  $p^*(q)$  and  $j^*(q)$ ,

$$p_i^*(q) = \begin{cases} \frac{q}{q^\pi} \pi_i & i \in \mathcal{S}, \\ \frac{1-q}{1-q^\pi} \pi_i & i \in \mathcal{N}, \end{cases}$$

$$j_{ij}^*(q) = \left[ \frac{q(1-q) + q^\pi(1-q^\pi)}{2q^\pi(1-q^\pi)} \right] j_{ij}^\pi. \quad (10)$$

Using this ansatz, we can bound  $I(q)$  according to

$$I(q) \leq I(p^*, j^*). \quad (11)$$

These particular  $p^*$  and  $j^*$  are simple choices that satisfy the constraints mentioned above, as well as  $j_{ij}^*(q^\pi) = j_{ij}^\pi$  and  $p_i^*(q^\pi) = \pi_i$ , ensuring that the inequality in Eq. (10) is saturated at the minimum,  $q = q^\pi$ . The coefficient in brackets in Eq. (10) was chosen to maximize the tightness of the bound on  $I(q)$ .

Following the approach of Ref. [39], inserting our choice of  $p^*$  and  $j^*$  into  $I(p, j)$  leads to an explicit upper bound on  $I''(q^\pi)$  in terms of the total energy consumption rate of the receptor (in units of  $k_B T$ ), defined as [27]

$$\Sigma^\pi = \sum_{i < j} j_{ij}^\pi \log \frac{\phi_{ij}^\pi}{\phi_{ji}^\pi}. \quad (12)$$

We then find a lower bound on the variance of  $q$  (see Sec. III of Ref. [45]):

$$\frac{\langle (\delta q)^2 \rangle}{[q^\pi(1-q^\pi)]^2} \geq \frac{8}{T \Sigma^\pi + 4\bar{N}}. \quad (13)$$

Equation (13) can be thought of as a general thermodynamic uncertainty relation which implies that the more energy  $T \Sigma^\pi$  a system consumes, the more reliable the occupation time for a pool of states can become. This can be compared to the thermodynamic uncertainty relation for currents, which connects increased energy consumption to a reduction in current fluctuations in general stochastic processes [39,40]. Our result in Eq. (13) adds pooled state occupancy times to the class of observables for which thermodynamic uncertainty relations can be generally proven and may, therefore, be of independent interest in nonequilibrium thermodynamics.

## VI. AN ENERGY-ACCURACY TRADEOFF FOR THE SIMPLE OBSERVER

The gain term  $c \frac{dq^\pi}{dc}$  in Eq. (8) can be calculated for arbitrary nonequilibrium processes using the known relationship between first passage times and the sensitivity of Markov chain stationary distributions [45,48]. Our general formulas

in Sec. IV of Ref. [45] simplify to

$$c \frac{dq^\pi}{dc} = q^\pi(1-q^\pi) \quad (14)$$

for nonequilibrium receptors of the form in Fig. 1(d) with only one nonsignaling state and binding transitions linear in  $c$ . The assumptions of one nonsignaling state and binding transitions that are linear in concentration are required at this stage of the derivation only. If the binding transition rates are related to concentration through a power law, the conclusions are similar (see Sec. VII of Ref. [45]). Inserting this result for gain and the relation for variance in Eq. (13) into Eq. (8), we find a general lower bound on error in terms of energy  $T \Sigma^\pi$  and mean binding events  $\bar{N}$ :

$$\epsilon_c^2 \geq \frac{8}{T \Sigma^\pi + 4\bar{N}}. \quad (15)$$

This recovers the Berg-Purcell limit, Eq. (1), for equilibrium systems, when the energy consumption rate  $\Sigma^\pi$  is zero.

Overall, Eq. (15) is a generalization of the Berg-Purcell limit, Eq. (1), to much more general energy consuming nonequilibrium receptors of the form in Fig. 1(d), with one nonsignaling (unbound) state, but an arbitrary network of signaling (bound) states. This LDT bound is clearly not tight as  $\Sigma^\pi \rightarrow \infty$ , but for finite  $\Sigma^\pi$  it provides a simple energy-based bound on error that is independent of both detailed number and the connectivity of receptor states. At  $\Sigma^\pi \geq 4\bar{N}/T$  the CR bound in Eq. (7) becomes more stringent than the LDT bound in Eq. (15), and any bound on the IO must also apply to the SO. Thus, the combined bound (the maximum of the CR and LDT bounds) yields a forbidden region of error versus energy [Fig. 2(a), top gray area].

## VII. EXACT ESTIMATION ERROR FOR THE SIMPLE OBSERVER

Equation (15) provides a lower bound on the fractional error because our choice of  $p^*$  and  $j^*$  in Eq. (10) does not achieve the infimum of the contraction. When the contraction of the rate function  $I(p, j)$  is expanded as a Taylor series in  $(q - q^\pi)$ , one can compute the optimal  $p$  and  $j$  to leading order, which allows us to find the second derivative term in the Taylor expansion of  $I(q)$  and hence the uncertainty  $\epsilon_c^2$  exactly (see Sec. V C of Ref. [45]). Under the same assumption of one nonsignaling state, we find

$$\epsilon_c^2 = \frac{2}{\bar{N}} \frac{T_{\text{unbind}}}{T_{\text{hold}}}, \quad \text{with}$$

$$T_{\text{hold}} = \sum_{i \in \mathcal{S}} \mathbf{T}_{i\mathcal{N}} \mathbb{P}(x(t) = i | x \text{ entered } \mathcal{S} \text{ at } t),$$

$$T_{\text{unbind}} = \sum_{i \in \mathcal{S}} \mathbf{T}_{i\mathcal{N}} \mathbb{P}(x(t) = i | x \text{ in } \mathcal{S} \text{ at } t). \quad (16)$$

Here  $\mathbf{T}_{i\mathcal{N}}$  is the mean first passage time from state  $i$  to the single nonsignaling state. Thus,  $T_{\text{hold}}$  is the mean duration of a single journey through the bound signaling states, starting from the time at which the bound signaling states are entered, and ending at the time at which the unbound nonsignaling state is first reached. Also  $T_{\text{unbind}}$  is the mean time until the next unbinding event given the receptor is in a bound signaling

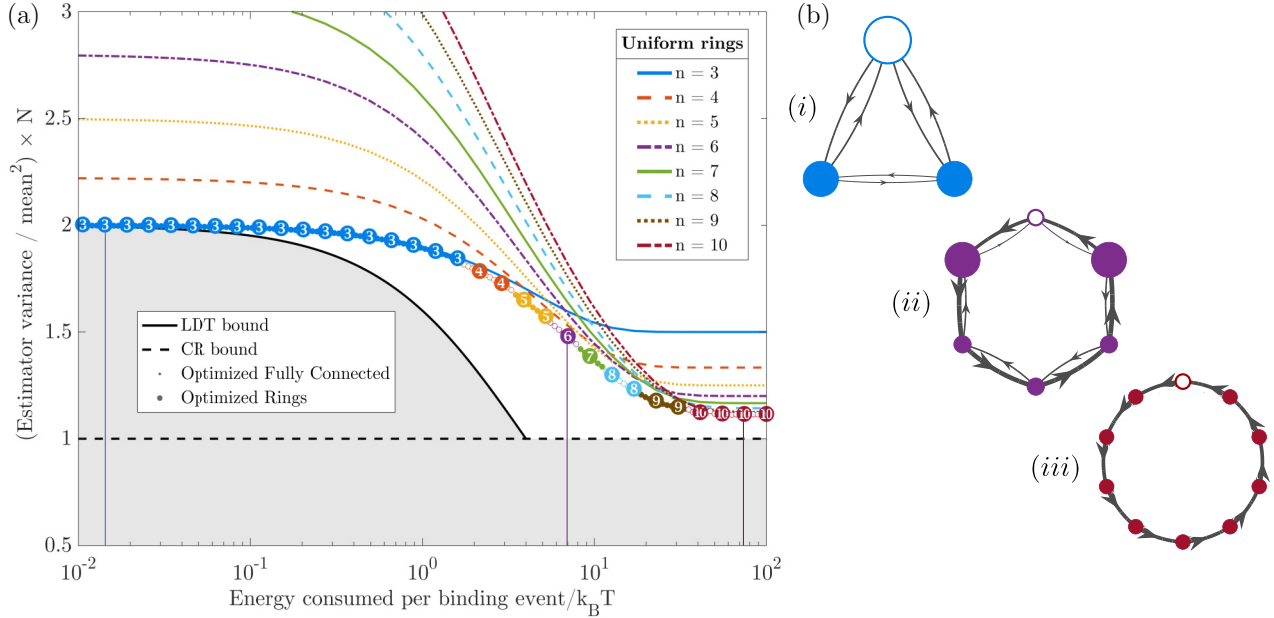


FIG. 2. Energy-accuracy tradeoffs: analytic bounds and numerical optimizations. (a) The LDT bound, Eq. (15) (solid black line), and the CR bound, Eq. (7) (dashed black line), together yield a forbidden region of achievable estimation error as a function of energy consumption (gray area). Circular points show the minimal error achieved by fully connected (small open and closed dots) and nonuniform ring (large numbered dots) receptors after numerically minimizing Eq. (16) (see Sec. V of Ref. [45]) with respect to all transition rates under an energy consumption constraint. The coincidence of small and large dots indicates that the much more general class of fully connected receptors does not outperform the simpler class of ring receptors with arbitrary nonuniform transition rates. Data point color and superposed numbers reflect the size of the smallest receptor whose error is within 1% of the fractional error of the best performing receptor obtained at each energy, with no constraint on overall size (up to a maximal size of  $n = 10$ ). Alternating open and solid small points represent the same effect for fully connected networks, and the numbers of nodes required agree with those indicated by the larger numbered ring network points in each open and solid region. The progression of colors and numbers as a function of energy indicates the smallest number of states required to achieve minimal error at that energy and shows that achieving even lower error at higher energy consumption cannot be done without adding more states. Thin solid, dashed, and dotted lines show the performance of  $n$ -state ring receptors with uniform transition rates in each direction. The lower performance envelope of the uniform ring receptors (obtained by minimizing over  $n$  at fixed energy consumption) is still separated from the better performing nonuniform rings and fully connected networks. This performance gap indicates that uniform rings cannot achieve the Pareto-optimal tradeoff between energy and accuracy. (b) Diagrams (i)–(iii) show three optimal receptors found at different levels of energy consumption indicated by the three vertical lines in panel (a). Low, intermediate, and high energy consumption levels correspond to blue three-state (i), purple six-state (ii), and red ten-state (iii) graphs, respectively. Solid nodes in the Markov chain diagrams (i)–(iii) represent signaling states, while one empty node at the top of each graph represents the nonsignaling state. Node radii are proportional to steady-state probabilities  $\pi_i$  and edge widths are proportional to steady-state fluxes between states,  $\phi_{ij}^+$ . These nonuniform rings illustrate how Pareto-optimal receptors reduce error by simultaneously increasing the number of states and the level of energy consumption, eventually approaching a uniform ring with many states at the highest levels of energy consumption.

state, regardless of how long the receptor has been bound before. In Sec. V C of Ref. [45] we have numerically verified this formula by comparing it with Monte Carlo simulations.

For a two-state system,  $T_{\text{unbind}} = T_{\text{hold}}$  because the unbinding process is memoryless; i.e., the time to unbind is independent of how long the receptor has already been bound. In this case, Eq. (16) saturates the Berg-Purcell limit in Eq. (1). However, Eq. (16) applies more generally to energy-consuming nonequilibrium receptors of the form in Fig. 1(d), with one nonsignaling state, but an arbitrary network of signaling states. While Eq. (16), and its generalization to multiple nonsignaling states (see Sec. V C of Ref. [45]), gives an exact formula for error that allows us to search for Pareto-optimal receptors, our LDT bound in Eq. (15) makes manifest a connection between estimation error and the energy consumption of the process.

### VIII. PARETO-OPTIMAL ERROR REDUCTION VIA ENERGY CONSUMPTION REQUIRES MORE STATES AND IS ACHIEVABLE BY RINGS

Figure 2 compares the bounds on estimation error in Eqs. (7) and (15) to numerical optimization of the exact formula (16) at fixed energy consumption for receptors of increasing size. The union of the CR and LDT lower bounds is respected by all models found by numerical optimization. First, for a given energy consumption and number of states  $n$ , we minimized the estimation error over all possible fully connected receptors, for every partition of  $n$  into signaling and nonsignaling states. We observed that, for all receptor sizes and energy consumption regimes studied, the error achieved by receptors with a single nonsignaling state is not outperformed by any other partitioning (see Fig. 6 in Sec. VI B of Ref. [45]). Therefore, we focused subsequent analyses on the

case of a single nonsignaling state. To explore the role of the total number of states  $n$  in the Pareto-optimal tradeoff between energy and accuracy, in Fig. 2 we numerically minimized the error over all possible fully connected receptors, including the number of states (up to ten), for a given energy consumption. We found that as energy consumption increases, near minimal estimation error is achievable only by increasing the number of states (see Fig. 4 of Ref. [45]).

In Sec. VI C of Ref. [45] we show that the numerically determined Pareto-optimal curves for a fixed number of states,  $n$ , are well approximated by the expression

$$\epsilon_c^2 = \frac{2}{\bar{N} \left[ 1 + \left( \frac{n-2}{n} \right) \tanh \left( \left\{ \frac{0.05n+0.06}{n-1.6} \right\} \frac{T \Sigma^\pi}{\bar{N}} \right) \right]}. \quad (17)$$

The coefficient in braces was determined by a least-squares fit to the numerical optima (see Sec. VI C of Ref. [45]).

The small graphs in Fig. 2(b) [diagrams (i)–(iii)] depict optimal minimal size receptors obtained at different levels of energy consumption. At low energy consumption the LDT bound is tight, and the optimal receptor is equivalent by lumpability [49] to a two-state receptor, with the signaling states behaving like one coarse-grained state (see Sec. VI A of Ref. [45]). In this low energy consumption limit there is no significant advantage gained by adding more than three states. The LDT bound, Eq. (15), becomes increasingly loose as energy consumption increases and the minimal achievable error of optimal receptors at fixed  $n$  saturates at a level that depends on the number of states. We can see from Fig. 2 that, as the energy consumption increases, there is an increasing advantage to adding more states beyond a two or three-state system. At intermediate energy consumption the optimal receptor behaves roughly like a three-state system, with “inner” states of  $\mathcal{S}$  being highly short-lived. At high energy consumption, the optimal receptor approaches a many-state uniform ring with more and more asymmetric transition rates at higher energies (see supplemental movies in Ref. [45]). As the number of states  $n \rightarrow \infty$ , the minimal achievable error at high energy consumption saturates the CR bound, Eq. (7). Thus, the combined LDT and CR bound is tight at both high and low energy consumption.

We repeated the optimization with receptors restricted to ring topologies with arbitrary transition rates and found that the best possible rings perform indistinguishably from fully connected networks at every energy level (Fig. 2(a)). This suggests that the Pareto-optimal tradeoff between energy and accuracy is achieved (but not uniquely) by nonuniform ring networks of increasing size and energy consumption. In the high energy consumption limit, however, only many-state, highly unidirectional ring processes are found to approach the theoretical limits [Fig. 2(b), diagram (iii)].

## IX. UNIFORM RING RECEPTORS ARE NOT PARETO-OPTIMAL

For ring receptors with uniform transition rates in each direction, we can analytically compute  $T_{\text{unbind}}$ ,  $T_{\text{hold}}$ , and therefore  $\epsilon_c^2$  in Eq. (16), as a function of  $n$ ,  $\Sigma^\pi$ , and  $\bar{N}$  (see Sec. V D

in Ref. [45]), obtaining

$$\epsilon_c^2 = \frac{n \coth \left[ \frac{\sigma}{2n} \right] \left( n \coth \left[ \frac{\sigma}{2} \right] - \coth \left[ \frac{\sigma}{2n} \right] \right)}{\bar{N} (n-1)^2}, \quad (18)$$

where  $\sigma$  is defined via  $\frac{\Sigma^\pi}{R^\pi} = \sigma \tanh \left[ \frac{\sigma}{2n} \right]$ . This error versus energy for  $n = 3, \dots, 10$  is plotted in Fig. 2. The lower envelope of these curves, corresponding to minimizing Eq. (18) with respect to  $n$  at fixed energy per binding event  $\frac{\Sigma^\pi}{R^\pi}$ , yields an upper bound on the numerically derived Pareto-optimal tradeoff. As seen in Fig. 2, at intermediate energy consumption, this upper bound is slightly higher than the minimal error achieved by nonuniform rings, indicating nonuniform transition rates are required for ring receptors to be optimal at intermediate energy. However, as  $\Sigma^\pi \rightarrow \infty$ ,  $\epsilon_c^2 \rightarrow \frac{1}{\bar{N}} \frac{1}{1-1/n}$ , indicating that a SO of uniform rings can approach the CR bound at large energy and  $n$ . The optimality of single path rings is reminiscent of the optimality of single path chains for hitting times, observed numerically in Ref. [50] for a different notion of energy. However, large uniform rings can be highly suboptimal under a SO at low energy; as  $\Sigma^\pi \rightarrow 0$ ,  $\epsilon_c^2 \rightarrow \frac{2}{\bar{N}} \frac{n(n+1)}{6(n-1)}$ . This saturates the Berg-Purcell limit in Eq. (1) for  $n = 2$  and 3, but is much worse for  $n > 3$  (Fig. 2). Therefore, larger uniform ring receptors *must* consume more energy to more closely approach the theoretical limit on estimation error, but adding additional states is only advantageous above a certain level of energy consumption. In summary, both receptor size and energy consumption must concomitantly increase in order to trace out the Pareto-optimal tradeoff between energy and accuracy, and this tradeoff can be achieved with nonuniform rings.

## X. DISCUSSION

In summary, we have derived several general results in the form of Eqs. (5), (7), (15), and (16) delineating fundamental performance limits of sensing using arbitrarily connected, energy-consuming nonequilibrium Markov chain receptors as a joint function of observation time, energy consumption rate, number of states, and the computational sophistication of the observer. Moreover we find a general thermodynamic uncertainty relation, Eq. (13), which reveals one must pay a universal energetic cost for reliable occupation time in any physical process. This relation may be compared to the thermodynamic uncertainty relation for currents, which was proved using similar methods but for a different physical observable [39]. We hope these general analytic relations between time, energy, and accuracy will find further applications in stochastic thermodynamics and myriad biological and physical processes [11, 12, 16, 43, 51–54]. Particularly, these types of theoretical bounds that do not depend on the details of the particular system could be useful in experimental interrogations of small out-of-equilibrium systems, where many degrees of freedom could be inaccessible to the observer [55].

## ACKNOWLEDGMENTS

S.E.H. was supported by the National Defense Science and Engineering Graduate Fellowship and the Stanford Graduate Fellowship. The authors thank the referees for their comments which helped improve the clarity of the manuscript. S.G. thanks the Simons Foundation and an NSF CAREER award for support.

- [1] C. U. M. Smith, *Biology of Sensory Systems*, 2nd ed. (Wiley-Blackwell, Hoboken, NJ, 2008).
- [2] V. Sourjik and N. S. Wingreen, Responding to chemical gradients: Bacterial chemotaxis, *Curr. Opin. Cell Biol.* **24**, 262 (2012).
- [3] W. Bialek, *Biophysics: Searching for Principles* (Princeton University, Princeton, NJ, 2012).
- [4] L. Song, S. M. Nadkarni, H. U. Bödeker, C. Beta, A. Bae, C. Franck, W. J. Rappel, W. F. Loomis, and E. Bodenschatz, Dictyostelium discoideum chemotaxis: Threshold for directed motion, *Eur. J. Cell Biol.* **85**, 981 (2006).
- [5] D. Ohtsuka, N. Ota, S. Amaya, S. Matsuoka, Y. Tanaka, and M. Ueda, A sub-population of *Dictyostelium discoideum* cells shows extremely high sensitivity to cAMP for directional migration, *Biochem. Biophys. Res. Commun.* **554**, 131 (2021).
- [6] J. D. Shields, M. E. Fleury, C. Yong, A. A. Tomei, G. J. Randolph, and M. A. Swartz, Autologous chemotaxis as a mechanism of tumor cell homing to lymphatics via interstitial flow and autocrine CCR7 signaling, *Cancer Cell* **11**, 526 (2007).
- [7] S. Fancher, M. Vennettilli, N. Hilgert, and A. Mugler, Precision of Flow Sensing by Self-Communicating Cells, *Phys. Rev. Lett.* **124**, 168101 (2020).
- [8] R. Landauer, Irreversibility and heat generation in the computing process, *IBM J. Res. Dev.* **5**, 183 (1961).
- [9] S. Laughlin, Energy as a constraint on the coding and processing of sensory information, *Curr. Opin. Neurobiol.* **11**, 475 (2001).
- [10] J. M. Horowitz and M. Esposito, Thermodynamics with Continuous Information Flow, *Phys. Rev. X* **4**, 031015 (2014).
- [11] J. M. R. Parrondo, J. M. Horowitz, and T. Sagawa, Thermodynamics of information, *Nat. Phys.* **11**, 131 (2015).
- [12] S. Lahiri, J. Sohl-Dickstein, and S. Ganguli, A universal tradeoff between power, precision and speed in physical communication, [arXiv:1603.07758](https://arxiv.org/abs/1603.07758).
- [13] P. Strasberg, G. Schaller, T. Brandes, and M. Esposito, Quantum and Information Thermodynamics: A Unifying Framework Based on Repeated Interactions, *Phys. Rev. X* **7**, 021003 (2017).
- [14] Y. Tu, The nonequilibrium mechanism for ultrasensitivity in a biological switch: Sensing by Maxwell's demons, *Proc. Natl. Acad. Sci. USA* **105**, 11737 (2008).
- [15] P. Mehta and D. J. Schwab, Energetic costs of cellular computation, *Proc. Natl. Acad. Sci. USA* **109**, 17978 (2012).
- [16] P. Mehta, A. H. Lang, and D. J. Schwab, Landauer in the age of synthetic biology: Energy consumption and information processing in biochemical networks, *J. Stat. Phys.* **162**, 1153 (2016).
- [17] P. B. Detwiler, S. Ramanathan, A. Sengupta, and B. I. Shraiman, Engineering aspects of enzymatic signal transduction: Photoreceptors in the retina, *Biophys. J.* **79**, 2801 (2000).
- [18] S. Ramanathan, P. B. Detwiler, A. M. Sengupta, and B. I. Shraiman, G-protein-coupled enzyme cascades have intrinsic properties that improve signal localization and fidelity, *Biophys. J.* **88**, 3063 (2005).
- [19] J. K. Weber, D. Shukla, and V. S. Pande, Heat dissipation guides activation in signaling proteins, *Proc. Natl. Acad. Sci. USA* **112**, 10377 (2015).
- [20] S. C. Erlandson, C. McMahon, and A. C. Kruse, Structural basis for G protein-coupled receptor signaling, *Annu Rev Biophys* **47**, 1 (2018).
- [21] H. C. Berg and E. M. Purcell, Physics of chemoreception, *Biophys. J.* **20**, 193 (1977).
- [22] W. Bialek and S. Setayeshgar, Physical limits to biochemical signaling, *Proc. Natl. Acad. Sci. USA* **102**, 10040 (2005).
- [23] K. Kaizu, W. de Ronde, J. Pajmans, K. Takahashi, F. Tostevin, and P. R. ten Wolde, The Berg-Purcell limit revisited, *Biophys. J.* **106**, 976 (2014).
- [24] T. Mora and N. S. Wingreen, Limits of Sensing Temporal Concentration Changes by Single Cells, *Phys. Rev. Lett.* **104**, 248101 (2010).
- [25] R. G. Endres and N. S. Wingreen, Maximum Likelihood and the Single Receptor, *Phys. Rev. Lett.* **103**, 158101 (2009).
- [26] A. H. Lang, C. K. Fisher, T. Mora, and P. Mehta, Thermodynamics of Statistical Inference by Cells, *Phys. Rev. Lett.* **113**, 148103 (2014).
- [27] U. Seifert, Stochastic thermodynamics: Principles and perspectives, *Eur. Phys. J. B* **64**, 423 (2008).
- [28] M. Esposito and C. Van den Broeck, Three faces of the second law. I. Master equation formulation, *Phys. Rev. E* **82**, 011143 (2010).
- [29] K. Sekimoto, *Stochastic Energetics*, Lecture Notes in Physics Vol. 799 (Springer, Berlin, 2010).
- [30] X.-J. Zhang, H. Qian, and M. Qian, Stochastic theory of nonequilibrium steady states and its applications. Part I, *Phys. Rep.* **510**, 1 (2012).
- [31] H. Ge, M. Qian, and H. Qian, Stochastic theory of nonequilibrium steady states. Part II: Applications in chemical biophysics, *Phys. Rep.* **510**, 87 (2012).
- [32] U. Seifert, Stochastic thermodynamics, fluctuation theorems, and molecular machines, *Rep. Prog. Phys.* **75**, 126001 (2012).
- [33] H. Touchette, The large deviation approach to statistical mechanics, *Phys. Rep.* **478**, 1 (2009).
- [34] C. Maes and K. Netočný, Canonical structure of dynamical fluctuations in mesoscopic nonequilibrium steady states, *Europhys. Lett.* **82**, 30003 (2008).
- [35] L. Bertini, A. Faggionato, and D. Gabrielli, Large deviations of the empirical flow for continuous time Markov chains, *Ann. Inst. H. Poincaré Probab. Statist.* **51**, 867 (2015).
- [36] L. Bertini, A. Faggionato, and D. Gabrielli, Flows, currents, and cycles for Markov Chains: Large deviation asymptotics, *Stoch. Process. Their Appl.* **125**, 2786 (2015).
- [37] A. C. Barato and R. Chetrite, A formal view on level 2.5 large deviations and fluctuation relations, *J. Stat. Phys.* **160**, 1154 (2015).
- [38] A. C. Barato and U. Seifert, Dispersion for two classes of random variables: General theory and application to inference of an external ligand concentration by a cell, *Phys. Rev. E* **92**, 032127 (2015).
- [39] T. R. Gingrich, J. M. Horowitz, N. Perunov, and J. L. England, Dissipation Bounds All Steady-State Current Fluctuations, *Phys. Rev. Lett.* **116**, 120601 (2016).
- [40] A. C. Barato and U. Seifert, Thermodynamic Uncertainty Relation for Biomolecular Processes, *Phys. Rev. Lett.* **114**, 158101 (2015).
- [41] J. M. Horowitz and T. R. Gingrich, Thermodynamic uncertainty relations constrain non-equilibrium fluctuations, *Nat. Phys.* **16**, 15 (2020).
- [42] G. Li and H. Qian, Kinetic timing: A novel mechanism that improves the accuracy of GTPase timers in endosome fusion and other biological processes, *Traffic* **3**, 249 (2002).

- [43] H. Qian, Phosphorylation energy hypothesis: Open chemical systems and their biological functions, *Annu. Rev. Phys. Chem.* **58**, 113 (2007).
- [44] R. Marsland, W. Cui, and J. M. Horowitz, The thermodynamic uncertainty relation in biochemical oscillations, *J. R. Soc. Interface* **16**, 20190098 (2019).
- [45] See Supplemental Material (SM) at <http://link.aps.org/supplemental/10.1103/PhysRevE.108.014403> for additional details and calculations, which includes [21,33–36,38,48,49,56–64]. It contains the full calculations summarized in this paper and also presents introductions to the theoretical methods employed in this paper for a physical sciences audience. Section II A of the SM details the Fisher information and maximum likelihood estimation calculations for the ideal observer case. Section III of the SM presents our calculation of a thermodynamic uncertainty principle for state densities, and Sec. IV of the SM computes the receptor gain. Section V of the SM contains exact calculations of the error for the ideal and simple observer cases. Section VI of the SM details our numerical methods used to generate Fig. 2, as well as presents numerical observations about the lumpability of optimized networks and networks with more than one nonsignaling state. Section VII of the SM discusses the extension to nonlinear transition rate dependence on concentration. Appendixes A and B of the SM are dedicated to an introduction to continuous-time Markov processes and large deviation theory for Markov processes. Appendix C gives descriptions of the supplemental movies which can be found in a Github repository at [https://github.com/ganguli-lab/Energy\\_Accuracy\\_Tradeoff\\_Cellular\\_Sensing](https://github.com/ganguli-lab/Energy_Accuracy_Tradeoff_Cellular_Sensing).
- [46] M. Skoge, S. Naqvi, Y. Meir, and N. S. Wingreen, Chemical Sensing by Nonequilibrium Cooperative Receptors, *Phys. Rev. Lett.* **110**, 248102 (2013).
- [47] T. M. Cover and J. A. Thomas, *Elements of Information Theory*, 2nd ed. (Wiley-Interscience, Hoboken, NJ, 2006), p. 748.
- [48] G. Cho and C. Meyer, Markov chain sensitivity measured by mean first passage times, *Linear Algebra Appl.* **316**, 21 (2000).
- [49] J. G. Kemeny and J. L. Snell, *Finite Markov Chains* (Springer, Berlin, 1960), p. 226.
- [50] S. Escola, M. Eisele, K. Miller, and L. Paninski, Maximally reliable Markov chains under energy constraints, *Neural Comput.* **21**, 1863 (2009).
- [51] G. Lan, P. Sartori, S. Neumann, V. Sourjik, and Y. Tu, The energy-speed-accuracy tradeoff in sensory adaptation, *Nat. Phys.* **8**, 422 (2012).
- [52] S. Still, D. A. Sivak, A. J. Bell, and G. E. Crooks, Thermodynamics of Prediction, *Phys. Rev. Lett.* **109**, 120604 (2012).
- [53] A. B. Boyd, D. Mandal, P. M. Riechers, and J. P. Crutchfield, Transient Dissipation and Structural Costs of Physical Information Transduction, *Phys. Rev. Lett.* **118**, 220602 (2017).
- [54] S. E. Marzen and J. P. Crutchfield, Prediction and dissipation in nonequilibrium molecular sensors: Conditionally Markovian channels driven by memoryful environments, *Bull. Math. Biol.* **82**, 25 (2020).
- [55] D. J. Skinner and J. Dunkel, Estimating Entropy Production from Waiting Time Distributions, *Phys. Rev. Lett.* **127**, 198101 (2021).
- [56] H. Cramér, *Mathematical Methods of Statistics* (Princeton University, Princeton, NJ, 1945), p. 575.
- [57] C. R. Rao, Information and the accuracy attainable in the estimation of statistical parameters, *Bull. Calcutta Math. Soc.* **37**, 81 (1945).
- [58] J. B. S. Haldane and S. M. Smith, The sampling distribution of a maximum-likelihood estimate, *Biometrika* **43**, 96 (1956).
- [59] D. D. Yao, First-passage-time moments of Markov processes, *J. Appl. Probab.* **22**, 939 (1985).
- [60] *MATLAB version 9.3.0.713579 (R2017b)*, The Mathworks, Inc., Natick, Massachusetts, 2017.
- [61] P. Virtanen, R. Gommers, T. E. Oliphant, M. Haberland, T. Reddy, D. Cournapeau, E. Burovski, P. Peterson, W. Weckesser, J. Bright, S. J. van der Walt, M. Brett, J. Wilson, K. Jarrod Millman, N. Mayorov, A. R. J. Nelson, E. Jones, R. Kern, E. Larson, C. Carey *et al.*, SciPy 1.0—Fundamental algorithms for scientific computing in Python, *Nat. Methods* **17**, 261 (2020).
- [62] J. H. Bollmann, B. Sakmann, and J. G. G. Borst, Calcium sensitivity of glutamate release in a Calyx-type terminal, *Science* **289**, 953 (2000).
- [63] R. Schneggenburger and E. Neher, Intracellular calcium dependence of transmitter release rates at a fast central synapse, *Nature (London)* **406**, 889 (2000).
- [64] J. Hunter, A survey of generalized inverses and their use in stochastic modelling, *Res. Lett. Inf. Math. Sci.* **1**, 25 (2000).